Drug Development and Industrial Pharmacy, 2010; 36(6): 724–734

informa
healthcare

ORIGINAL ARTICLE

The influence of chirality, physicochemical properties, and permeation enhancers on the transdermal permeation of amlodipine across rat skin

Aiguo Zeng[1], Changhe Wang[2], Bingxiang Yuan[1], Guangde Yang[1] and Qiang Fu[1]

[1]*School of Medicine, Xi'an Jiaotong University, Xi'an, PR China and* [2]*Shaanxi Institute for Food and Drug Control, Xi'an, PR China*

Abstract

Purpose: This study was aimed at investigating the possible relationship between the physical properties and the permeation of *S*-amlodipine and *RS*-amlodipine and studying the possible enantioselectivity of permeation of amlodipine in the presence and absence of enhancers, such as terpene enhancers and ethanol. *Method*: The solubility of *S*-amlodipine and *RS*-amlodipine was measured using the shake-flask method. The thermodynamic properties were investigated by differential scanning calorimetry (DSC). The type of racemate amlodipine was investigated by DSC and Fourier transform infrared spectroscopy (FTIR). The permeability of racemate and enantiomers of amlodipine through rat epidermis in vitro was investigated using the modified Franz diffusion cell. *Results*: The aqueous solubility of *S*-amlodipine was higher than that of *RS*-amlodipine. The melting temperature and enthalpy of fusion of *S*-amlodipine were lower than those of *RS*-amlodipine. *RS*-amlodipine was a racemic compound. The permeation of the enantiomers of amlodipine from *RS*-amlodipine reservoir showed no significant differences in the presence and absence of enhancers, but the permeation of *S*-amlodipine from *S*-amlodipine reservoir was significantly higher than that of *RS*-amlodipine from *RS*-amlodipine reservoir 30% ethanol, 50% ethanol, and terpene enhancers could not influence the difference in permeation between *S*-amlodipine and *RS*-amlodipine, but 75% ethanol could reduce the difference. *Conclusion*: These results suggested that there was no enantioselectivity of the enantiomers of amlodipine from *RS*-amlodipine reservoir in the presence and absence of enhancers, but the differences in physical properties between *S*-amlodipine and *RS*-amlodipine led to the difference in permeation across rat skins.

Key words: *Amlodipine; chirality; ethanol; physicochemical properties; skin permeation; terpene*

Introduction

Characterization of chiral drugs is attracting a great deal of attention from manufacturing and regulatory organizations, because the opposite enantiomer of a chiral drug often differs significantly in its pharmacological, toxicological, pharmacodynamic, and pharmacokinetic properties[1–5]. Furthermore, the chirality of a drug also influences the efficiency of delivery, which has not been well recognized in the pharmaceutical field. From a pharmaceutical perspective, the physical properties of both the racemate and the enantiomer, such as solubility and thermodynamic properties, should be characterized in detail for developing a safe, efficacious, and reliable formulation, no matter whether the racemate or the enantiomer is chosen as the marketed form. Because many physical properties of a crystalline solid are governed by the crystal structure, understanding the crystal structure of the racemate may explain the difference in the physical properties between the enantiomers and the racemate. A crystalline racemate may exist as a conglomerate, a racemic compound, or a pseudoracemate[6]. A racemic conglomerate is an equimolar eutectic mixture consisting of crystals of the two opposite enantiomers, with each crystal containing homochiral molecules. A racemic compound is a

Address for correspondence: Prof. Qiang Fu, School of Medicine, Xi'an Jiaotong University, Xi'an 710061, PR China. Tel: +86-029-82655382. E-mail: fuqiang@mail.xjtu.edu.cn

(Received 3 Mar 2009; accepted 2 Nov 2009)

ISSN 0363-9045 print/ISSN 1520-5762 online © Informa UK, Ltd.
DOI: 10.3109/03639040903460438

cocrystal containing equal numbers of molecules of the opposite enantiomer, usually paired up, with the unit cell of each crystal containing enantiomeric molecules with opposite chirality. Additionally, a racemic compound possesses different physical properties from those of the enantiomers. By contrast, a pseudoracemate is a solid solution containing equal numbers of molecules of the opposite enantiomers in a more or less random arrangement. Different types of racemic species can be distinguished by differential scanning calorimetry (DSC), X-ray powder diffractometry, and Fourier transform infrared spectroscopy (FTIR)[7,8].

In the last decade, the transdermal delivery of chiral drugs is an increasingly active and promising field because of the differences in permeation among the different stereoforms of chiral drugs. On the one hand, the stratum corneum, the rate-limiting barrier to percutaneous absorption, is made up of keratin and ceramides that could potentially provide a chiral environment. Differential binding of chiral drug enantiomers to keratin or interactions with ceramide may give rise to differences in the permeation profiles[9]. Miyazaki et al.[10] had reported that the flux of the *S*-propranolol-free base across excised rat skin in vitro was higher than that of the *R*-propranolol. Stereoselective processes were also observed within the viable epidermis in contact with dermatitis and in skin metabolism related to skin enzymatic activity[11–13]. Furthermore, skin permeation enhancers, especially chiral terpene enhancers, may also be implicated in enantioselective permeation. It was reported that the permeation enhancing effect of L-menthol on *S*-metoprolol-free base was significantly higher (by 25%) than that on *R*-metoprolol-free base across hairless mouse skin[14]. However, no significant differences were reported for the enantiomers of ketoprofen[8]. So, the enantioselective permeation of chiral drug enantiomers should be investigated further.

On the other hand, the differences in the physical properties between enantiomers and the racemate may also implicate the differences in permeation between enantiomers and the racemate[15,16]. Enantiomers with a lower melting point may exhibit higher solubility than that of the racemate and consequently have higher skin permeation profiles. Touitou et al. reported that the enantiomer of nivaldipine has a lower melting point by 34°C compared with the racemate and that the flux of the enantiomer across human cadaver skin was about sevenfold higher than that of the racemate[16]. But, in the case of ketorolac[17], the racemate has higher solubility by twofold and lower melting point by 20°C compared with the enantiomer, and the skin flux of the racemic compound was about 1.5-fold higher than those of the enantiomers. So, understanding the possible interrelationship between physical properties and enantiomeric interactions of chiral molecules in the crystalline state may offer explanation to the difference in permeation between the enantiomers and the racemate.

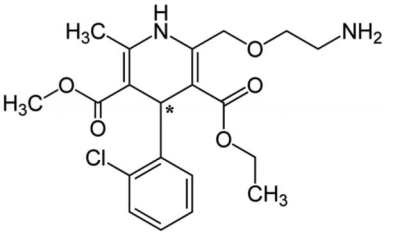

Figure 1. The structure of amlodipine. The asterisk denotes the chirality center in the molecule.

Amlodipine, (*R,S*)-2-[(2-aminoethoxy)methyl]-4-(2-chlorophenyl)-ethoxycarbonyl-5-methoxycarbonyl-6-methyl-1,4-dihydropyridine (Figure 1), is a potent calcium channel blocker used in the treatment of hypertension and angina pectoris[18–20]. Like most other calcium blocker agents of the dihydropyridine type, amlodipine molecule contains one chiral center, and the vasodilating effect only resides in the *S*-enantiomer[21,22]. It was reported that the elimination of amlodipine in urine was slightly enantioselective[4]. Although there has been much work done on the development of transdermal systems[23,24], there were no reports on stereoselective permeation of amlodipine enantiomers.

In this study, the objective was to investigate the possible relationship between the physical properties and the permeation of *S*-amlodipine and racemate amlodipine and to study the possible enantioselectivity of permeation of amlodipine in the presence and absence of enhancers, such as terpene enhancers and ethanol. It is hypothesized that the difference in permeation between the enantiomers and the racemate depends on the physical properties of the enantiomers and racemate, and there is possibly enantioselectivity in the permeation of chiral drugs across rat skin. Specifically, the physical properties of *S*-amlodipine and racemate amlodipine were determined, such as solubility, thermodynamic properties, and racemic species; and the permeation of *S*-amlodipine and racemate amlodipine across rat skin in vitro was determined using the modified Franz diffusion cell in the presence and absence of enhancers.

Materials and methods

Chemicals

S-amlodipine and *RS*-amlodipine were obtained from Cangzhou Senary Chemical Science-Tech Co., Ltd. (Cangzhou, Hebei, China); (–)-menthol, (–)-limonene, and linalool were purchased from Tokyo Kasei Kogyo

Co., Ltd. (Tokyo, Japan); 1-octanol from Tianjin Hongyan Chemical Reagent Factory (Tianjin, China); high-performance liquid chromatography (HPLC)-grade acetonitrile and L-propanol from Fisher Scientific (Pittsburgh, PA, USA); spectral grade potassium bromide from Tianjin Fuchen Chemical Reagent Factory (Tianjin, China); and other reagents used in the experiment were analytical grade and from commercial sources.

Animals

Female Sprague–Dawley rats (5–7 weeks old) were supplied by the Experimental Animal Centre of Xi'an Jiaotong University (Xi'an, China). All experimental protocols involving animals were reviewed and approved by the Institutional Animal Experimentation Committee of Xi'an Jiaotong University.

Solubility

The solubility of *S*-amlodipine and *RS*-amlodipine was determined in water using the shake-flask method. Excess of *S*-amlodipine or *RS*-amlodipine was placed into a 25-mL conical flask containing 10 mL of water, and then the conical flasks were sealed tightly. The samples were shaken by an HZ-881S action shaker (Taicang City Scientific Instruments Factory, Taicang, China) in a water bath for 48 hours at 37°C. After shaking for 48 hours, the supernatant was then filtered through a 0.22-μm millipore membrane filter and the filtrate was diluted in ethanol. The concentration of *S*-amlodipine and *RS*-amlodipine in the diluted solution was measured by HPLC.

1-Octanol/water partition coefficients

The 1-octanol/water partition coefficients of *S*-amlodipine and *RS*-amlodipine were measured using the shake-flask method. The accurately weighed *S*-amlodipine or *RS*-amlodipine was dissolved in 10 mL of 1-octanol saturated with water. This solution was then added to 10 mL of water saturated with 1-octanol. The mixture of the two solvents was oscillated by an HZ-881S action shaker (Taicang City Scientific Instruments Factory) in a water bath for 24 hours at 37°C. After shaking, samples were centrifuged for 10 minutes to ensure that any emulsions were removed. An appropriate volume of each phase was taken and the 1-octanol phase was diluted with ethanol. *S*-amlodipine or *RS*-amlodipine concentrations of each ethanol/1-octanol and water solutions were measured by HPLC. The partition coefficients were calculated according to the ratio C_{oct}/C_{water}, where C_{oct} and C_{water} are the concentrations of the drug in 1-octanol and in water, respectively.

Thermal analysis

Thermoanalytical studies were performed with a DSC822[e] (Mettler Toledo, Zurich, Switzerland). The samples were scanned from 25°C to 200°C at the rate of 10°C/min under nitrogen atmosphere. The DSC curves were recorded and analyzed using the STAR[e] software. Temperatures and enthalpies were calibrated using indium phase transition (99.99% pure; heat of fusion, 28.45 J/g; melting point, 429.76 K). The enantiomeric mixtures with mole fractions of *S*-amlodipine between 0.5 and 1.0 were prepared by dissolving accurately weighed quantities of *RS*-amlodipine and *S*-amlodipine in methanol. The resultant solutions were vortex mixed, and the methanol was evaporated thoroughly at 40°C under vacuum. The obtained crystalline residues were annealed at room temperature for 36 hours. The samples (3–4 mg) were accurately weighed directly into aluminum pans. The pans were then covered with lids and sealed using the crucible sealing press (Mettler Toledo). Before each scan, a baseline was recorded with the same heating rate and then subtracted from the experimental scan.

Infrared spectroscopy

Infrared spectra were recorded in the range 4000–450/cm with an FTIR spectrophotometer (FTIR-8400S; Shimadzu, Tokyo, Japan) on KBr pellets using 32 scans for each sample with a resolution factor of 4. The spectra were corrected by subtracting the spectrum of a KBr blank pellet and presented in the transmittance mode.

Transdermal permeation studies

Rat epidermis was used for the transdermal penetration studies in vitro. The female Sprague–Dawley rats were killed by cervical dislocation after their hair had been removed with an electric clipper (900; TGC Inc., Tokyo, Japan) and full thickness skin was excised from the abdomen. The epidermis was then prepared by a heat separation technique. The whole skin was soaked in water at 60°C for 45 seconds, followed by careful removal of the epidermis. The epidermis was washed with water and used for permeability studies in vitro. The rat epidermis was mounted onto the modified Franz diffusion cell with the stratum corneum side facing toward the donor compartment, with an effective diffusion area of 1.54 cm^2 and a receptor compartment volume of 17.5 mL. Ethanol (30%, v/v) was added to the receiver cell to maintain sink conditions. The donor vehicle consisted of water or ethanol–water systems, and the donor compartment was filled with 0.02 M or a saturated solution of *S*-amlodipine or *RS*-amlodipine in the presence and absence of permeation enhancers. Cells were maintained at 37 ± 0.5°C using a water bath

circulator. The contents in the receiver compartment were stirred with the help of a magnetic bar rotating at 600 rpm during the experiment. The permeate samples were withdrawn from the receiver compartment at different time intervals up to 12 hours, and an equivalent volume of drug-free solvent was added to the receiver compartment to maintain a constant volume. The permeate samples were then analyzed by HPLC for racemate and enantiomers of amlodipine content.

HPLC analyses

RS-amlodipine from the *RS*-amlodipine reservoir and *S*-amlodipine from the *S*-amlodipine reservoir in the transdermal penetration studies were determined by a nonchiral RP-HPLC method. The HPLC system consisted of an SCL-10A vp system controller, an LC-10AT vp liquid chromatograph, and an SPD-10A vp UV–Vis detector set at the wavelength of 237 nm (all from Shimadzu). The analytical column was a kromasil C_{18} (150 × 4.6 mm ID, 5 µm). The mobile phase was a mixture of water containing 30 mM potassium dihydrogen phosphate and acetonitrile (65:35, v/v) and the flow rate was 1.0 mL/min. The retention time was approximately 7.5 minutes. The HPLC assay was validated for specificity, linearity, and precision.

Amlodipine enantiomers from the *RS*-amlodipine reservoir in the transdermal penetration studies were determined by a previously reported stereospecific HPLC method[25,26], with the same the HPLC system adopted as above. The chiral stationary phase used to determine amlodipine enantiomers was a Chiral-AGP column (150 × 4.6 mm ID) packed with α_1-acid glycoprotein coated on silica (5 µm) from Chromtech (Congleton, Cheshire, UK). The mobile phase was a mixture of 10 mM ammonium acetate buffer (pH 4.5) and 1-propanol (99:1, v/v) with a flow rate of 0.9 mL/min. Under the specified conditions, baseline separation of amlodipine enantiomers was obtained. The retention time of *S*-amlodipine and *R*-amlodipine was approximately 17.5 and 22.5 minutes, respectively. The stereospecific HPLC method was validated for specificity, enantioresolution, linearity, and precision.

Data analysis

The steady-state skin flux was determined using Fick's law of diffusion:

$$J_s = \left(\frac{1}{A}\right)\left(\frac{dQ}{dt}\right), \quad (1)$$

where J_s is the steady-state flux (µg/cm^2/h), dQ/dt is the amount of drug permeated in unit time, and A is the diffusion area (cm^2). J_s was determined from the linear portion of the plot of cumulative amount permeated per unit area versus time. The lag time was determined by extrapolating the linear portion of the curve to the abscissa.

The effectiveness of the permeation enhancer was evaluated using enhancement ratio:[27]

$$ER_{flux} = \frac{\text{the steady-state flux of the drug with the enhancer}}{\text{the steady-state flux of the same drug without the enhancer}}, \quad (2)$$

where ER_{flux} is the enhancer ratio. Statistical differences were established by one-way analysis of variance and considered significant at $P < 0.05$.

Results and discussion

Physical properties

Solubility and the partition coefficients

The solubility and the partition coefficients of *S*-amlodipine and *RS*-amlodipine were different as listed in Table 1. The aqueous solubility of *S*-amlodipine was higher than that of *RS*-amlodipine. The observed partition coefficients of *S*-amlodipine and *RS*-amlodipine were determined using 1-octanol/water at 37°C and corrected for fractional dissociation to give log *P* values of 2.95 ± 0.09 and 2.89 ± 0.12, respectively. The difference in the partition coefficients between enantiomer and racemate was not significant.

Melting point and enthalpy of fusion

Thermal characteristics of *S*-amlodipine and *RS*-amlodipine were measured by DSC. Representative DSC scans of *S*-amlodipine and *RS*-amlodipine were given in Figure 2, and the thermodynamic data were shown in Table 1. *S*-amlodipine and *RS*-amlodipine exhibited single endotherm before melting, which suggested that they do not undergo any solid-state alterations up to their respective melting points. *RS*-amlodipine

Table 1. Physical properties of the *RS*-amlodipine and *S*-amlodipine.

Parameter	*RS*-amlodipine	*S*-amlodipine
Solubility in water (µg/mL)	67.8 ± 3.4	82.3 ± 4.8
log *P*	2.89 ± 0.12	2.95 ± 0.09
T_m (K)	414.32 ± 0.36	384.22 ± 0.42
ΔH^f (kJ/mol)	20.22 ± 0.27	16.86 ± 0.14

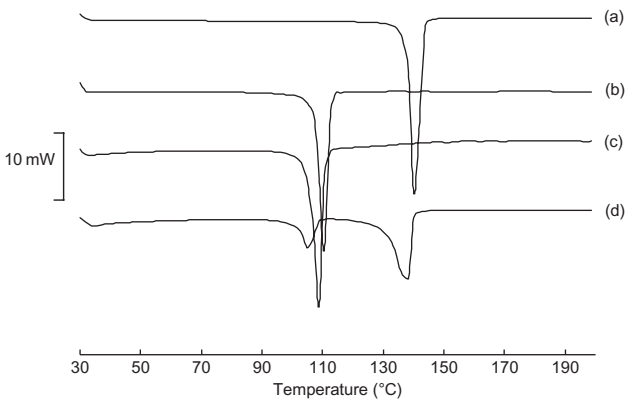

Figure 2. DSC curves of *RS*-amlodipine, *S*-amlodipine, and the mixture of *S*-amlodipine and *RS*-amlodipine: (a) *RS*-amlodipine, (b) *S*-amlodipine, (c) *S*-amlodipine:*RS*-amlodipine (0.895:0.105), (d) *S*-amlodipine:*RS*-amlodipine (0.294:0.706).

had higher melting point (T^f) and higher enthalpy of fusion (ΔH^f) than those of *S*-amlodipine.

The binary phase equilibrium diagram

To characterize the type of racemic compound, the binary phase equilibrium diagram was determined by DSC. Representative DSC scans of various samples of amlodipine were given in Figure 2. The *S*-amlodipine and *RS*-amlodipine exhibited single endotherms whereas disproportionate mixtures of enantiomers exhibited two endotherms. The binary phase equilibrium diagram (Figure 3) suggested that *RS*-amlodipine is a molecular complex and a racemic compound, which is characterized by a crystal form in which two

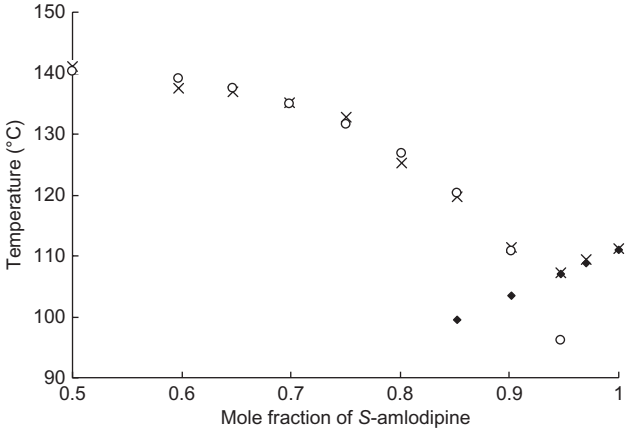

Figure 3. Melting point phase diagram of amlodipine enantiomers showing racemic compound formation between *S*- and *R*-amlodipine. The following are the symbol representations: (×) experimentally measured temperatures of complete melting; (○) values predicted by the Prigogine–Defay equation; and (♦) values predicted by the Schröder–van Laar equation.

enantiomers coexist in the same unit cell. In this type of racemic modification, the affinity between *R*- and *S*-amlodipine was greater than that between the same enantiomers. In such cases, *R*- and *S*-enantiomers paired up in the unit cell of the crystal that contains an equal number of the two antipodes. Then, the binary phase equilibrium diagram was calculated. The liquidus line between the pure enantiomer and the eutectic point was calculated by the Schröder–van Laar equation (Equation 3). The liquidus line between the racemic compound and the eutectic point was calculated by the Prigogine–Defay equation (Equation 4).

$$\ln x = \frac{\Delta H_S^f}{R}\left(\frac{1}{T_S^f} - \frac{1}{T^f}\right) \tag{3}$$

$$\ln 4x(1-x) = \frac{2\Delta H_{RS}^f}{R}\left(\frac{1}{T_{RS}^f} - \frac{1}{T^f}\right), \tag{4}$$

where x is the mole fraction of the more abundant enantiomer, with ΔH_{RS}^f and ΔH_S^f representing the enthalpy of fusion of the racemic compound and the enantiomer, respectively, and T_{RS}^f, T_S^f, and T^frepresenting the melting points of the racemic compound, the enantiomer, and the solid mixture, respectively. The DSC observations on various enantiomeric compositions of amlodipine were in good agreement with the liquidus curve predicted using Equations (3) and (4), as shown in Figure 3. Furthermore, if $\ln x\,(1-x)$ was plotted against the experimental values of $1/T^f$ (where T^f is determined by DSC), a straight line was obtained whose slope gave the calculated enthalpy of fusion (ΔH_R^f) for the racemic compound[28]. For *RS*-amlodipine, the plot was linear with the slope (ΔH_R^f) value of 22.71 kJ/mol that was comparable with the value 20.22 kJ/mol, obtained directly from the area under the DSC melting endotherm of *RS*-amlodipine. So, the binary phase equilibrium diagram of *RS*-amlodipine confirmed the racemic compound character.

Petterson proposed a definition of racemic compound stability based on the definition of the i value, that is, the difference between racemic compound and eutectic melting points divided by the difference between enantiomer and eutectic melting points[29]. An i value <0.5 would indicate only a weak tendency to form a racemic compound, whereas i value >1.5 would indicate a strong tendency to do so. The binary phase equilibrium diagram (Figure 3) showed eutectic behavior, the eutectic composition corresponds to a mole fraction x=92.27% with a melting point value of 378.27 K. According to Petterson's rule, therefore, the calculated

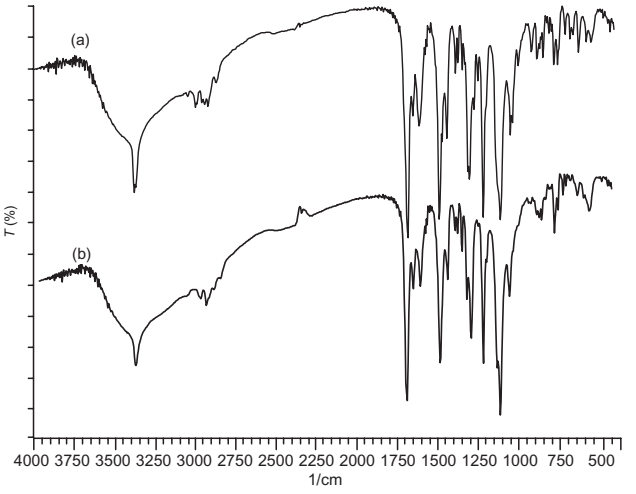

Figure 4. FTIR spectra of *S*-amlodipine and *RS*-amlodipine: (a) *S*-amlodipine, (b) *RS*-amlodipine.

i value for amlodipine ($i = 6.06$) would indicate a strong tendency to form a racemic compound.

Fourier-transform infrared spectroscopy

The FTIR spectra of *S*-amlodipine and *RS*-amlodipine were shown in Figure 4. There were substantial differences between the FTIR spectra of *S*-amlodipine and *RS*-amlodipine. *RS*-amlodipine did not show the bands (1465, 1267, 1186, 1027, and 993/cm) presented in the single enantiomer, but presented infrared bands (1309 and 1118/cm) lacking in the single enantiomer. Differences were also present between 3040 and 2860/cm (where there was a broad complex absorption because of superimposing C–H stretching vibrations of the methyl and methylene groups) and between 900 and 540/cm. Most bands highly characteristic of the molecular skeletal structure were essentially unchanged, for example, 3369/cm (N–H stretching vibrations of the primary amine), 1685/cm (C = O stretching vibrations of the ester), 1647/cm (C = C stretching vibrations), 1608 and 1481/cm (bands due to skeletal stretching vibrations of the benzene ring), and 1294, 1209, and 1105/cm (bands due to C–N stretching vibrations of the saturated alkyl nitrile or C–O stretching vibrations of the ether). The fact that the infrared spectra of the *S*-amlodipine differed markedly from that of *RS*-amlodipine demonstrates clearly that they possessed different crystal structures and that therefore *RS*-amlodipine existed as racemic compounds.

The binary phase equilibrium diagram and infrared spectra confirmed that the crystalline of *RS*-amlodipine existed as racemic compounds. The racemic amlodipine was a cocrystal containing equal numbers of molecules of the opposite enantiomer, usually paired up, with the unit cell of each crystal containing the heterochiral molecules. By contrast, *S*-amlodipine was a crystal containing the same *S*-enantiomers, with the unit cell of each crystal containing the homochiral molecules. In this type of racemic modification, the affinity between *R*- and *S*-amlodipine was greater than that between the same enantiomers. The differences in interactions between the same homochiral molecules and those between the heterochiral molecules and the different packing arrangements in the crystal structures led to the differences in physical properties between *S*-amlodipine and *RS*-amlodipine, such as solubility, melting point, and enthalpy of fusion.

Permeation of S-amlodipine and RS-amlodipine from saturated water solution

The permeation profiles of the racemate and enantiomers of amlodipine through the rat epidermis from saturated water solution of *S*-amlodipine or *RS*-amlodipine were shown in Figure 5. The permeation parameters were summarized in Table 2. The permeation profiles of *R*-amlodipine and *S*-amlodipine from *RS*-amlodipine reservoir were found to be comparable with the flux values of 3.96 ± 0.57 and 3.86 ± 0.46 μg/cm^2/h, respectively ($P > 0.05$), with the ratio of the flux values of *S*-amlodipine and *R*-amlodipine being 1.03 ± 0.06. No racemization was observed during the permeation process. These results suggested that the chiral nature of the stratum corneum and epidermis does not give rise to enantioselective permeation. These findings were in agreement with the reported studies on ketoprofen, ephedrine, and metoprolol, where no enantioselective permeation across the skin was observed[8,9,14]. It is speculated that the number of stereoselective sites in the skin may be limited

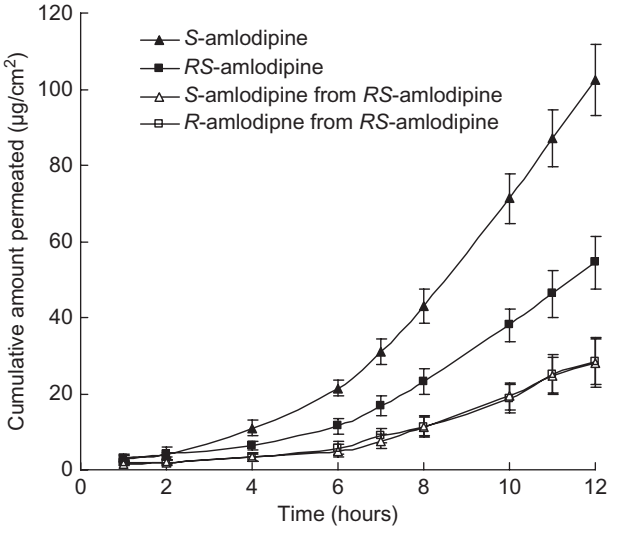

Figure 5. Permeation profiles of the racemate and enantiomers of amlodipine through the rat epidermis from water saturated with either *S*-amlodipine or *RS*-amlodipine.

Table 2. Permeation parameters of the racemate and enantiomers of amlodipine through the rat epidermis employing the donor phase consisting of *S*-amlodipine or *RS*-amlodipine in the water and ethanol–water systems.

Donor composition	Permeant	J_s (μg/cm^2/h)	T_{Lag} (h)	ER_{flux}	Ratio *S/R* or *S/RS*
Water + *S*-amlodipine	*S*-amlodipine	13.69 ± 1.41	4.66 ± 0.52		1.89 ± 0.15
Water + *RS*-amlodipine	*RS*-amlodipine	7.24 ± 1.02	4.62 ± 0.58		
	S-amlodipine	3.96 ± 0.57	4.97 ± 0.61		1.03 ± 0.06
	R-amlodipine	3.86 ± 0.46	4.75 ± 0.57		
30% Ethanol + *S*-amlodipine	*S*-amlodipine	21.12 ± 2.08	3.74 ± 0.42	1.54 ± 0.32	2.04 ± 0.19
30% Ethanol + *RS*-amlodipine	*RS*-amlodipine	10.35 ± 1.14	3.85 ± 0.49	1.43 ± 0.27	
	S-amlodipine	4.88 ± 0.63	3.62 ± 0.39		0.98 ± 0.05
	R-amlodipine	4.96 ± 0.57	3.57 ± 0.41		
50% Ethanol + *S*-amlodipine	*S*-amlodipine	28.25 ± 3.16	2.79 ± 0.33	2.06 ± 0.18	1.91 ± 0.24
50% Ethanol + *RS*-amlodipine	*RS*-amlodipine	14.83 ± 1.54	2.92 ± 0.25	2.04 ± 0.21	
	S-amlodipine	7.22 ± 0.85	3.02 ± 0.32		1.02 ± 0.06
	R-amlodipine	7.45 ± 0.79	2.91 ±0.28		
75% Ethanol + *S*-amlodipine	*S*-amlodipine	7.73 ± 1.12	0.25 ± 0.34	0.56 ± 0.08	1.38 ± 0.11
75% Ethanol + *RS*-amlodipine	*RS*-amlodipine	5.62 ± 1.03	0.74 ± 0.29	0.78 ± 0.11	
	S-amlodipine	2.80 ± 0.44	0.77 ± 0.28		1.02 ± 0.07
	R-amlodipine	2.76 ± 0.39	0.60 ± 0.24		

and, therefore, may not have contributed to any enantioselective permeation at the drug concentrations used. When donor solution contained either *RS*-amlodipine or *S*-amlodipine, the flux values of *S*-amlodipine and *RS*-amlodipine from water were 13.69 ± 1.41 and 7.24 ± 1.02 μg/cm^2/h, respectively ($P < 0.05$), with the ratio of the flux values of *S*-amlodipine and *RS*-amlodipine being 1.89 ± 0.15. These results showed significant difference between *S*-amlodipine and *RS*-amlodipine.

A simple relationship between the ratio of permeation fluxes and melting temperatures, referred to as melting temperature-membrane transport, was proposed by Touitou et al. in the early 1990s[16]. Based on their thermodynamic characteristics (Table 1) discussed in the earlier sections, the flux ratio of *S*-amlodipine versus *RS*-amlodipine from their saturated water solutions could be predicted using the following melting temperature-membrane transport mathematical model:

$$\ln\left(\frac{F_{\max S}}{F_{\max RS}}\right)=\frac{\Delta H^f_{RS}(T^f_{RS}-T)}{RT^f_{RS}T}-\frac{\Delta H^f_{S}(T^f_{S}-T)}{RT^f_{S}T},$$

where T equals 310.15 K, F_{max} represents the flux value when the donor vehicle is saturated with drug, and other terms can be interpreted as described in earlier sections. According to the above equation one could predict that *S*-amlodipine would have 2.03-fold higher F_{max} value than that of *RS*-amlodipine. The observed F_{max} ratio was 1.89 and in close agreement with the predicted values. Therefore, in this study, the difference in the physical properties (melting point, enthalpy of fusion, and solubility) gave rise to the difference of the permeation flux of *S*-amlodipine and *RS*-amlodipine from water.

Effect of ethanol on permeation of S-amlodipine and RS-amlodipine

The permeation profiles of the racemate and enantiomers of amlodipine through the rat epidermis from ethanol–water system containing *S*-amlodipine or *RS*-amlodipine were shown in Figure 6. The permeation parameters were summarized in Table 2. The permeation profiles of *R*-amlodipine and *S*-amlodipine from *RS*-amlodipine reservoir were found to be comparable with the ratios of the flux values of *S*-amlodipine and *R*-amlodipine from 30% ethanol, 50% ethanol, and 75% ethanol being 0.98 ± 0.05, 1.02 ± 0.06, and 1.02 ± 0.07, respectively. These results showed that ethanol in the donor solution did not give rise to any enantioselective permeation.

When donor solution contains either *RS*-amlodipine or *S*-amlodipine, the differences of *S*-amlodipine and *RS*-amlodipine were still significant, with the ratios of the flux values of *S*-amlodipine and *RS*-amlodipine from 30% ethanol, 50% ethanol, and 75% ethanol being 2.04 ± 0.19, 1.91 ± 0.24, and 1.38 ± 0.11, respectively. Compared with the ratios of the flux values of *S*-amlodipine and *RS*-amlodipine from water, 30% ethanol and 50% ethanol did not influence the ratios of the flux values of *S*-amlodipine and *RS*-amlodipine, whereas 75% ethanol could decrease the ratio of the flux values of *S*-amlodipine and *RS*-amlodipine. The result could be explained as follows. A high concentration of ethanol (75%) caused protein denaturation in skin, so that it behaved like a porous membrane that was unable to distinguish drug polarity[30]. So, 75% ethanol decreased the ratio of the flux values of *S*-amlodipine and *RS*-amlodipine.

The flux values of *S*-amlodipine and *RS*-amlodipine from water and ethanol–water system containing *S*-amlodipine or *RS*-amlodipine were evaluated. Table 2

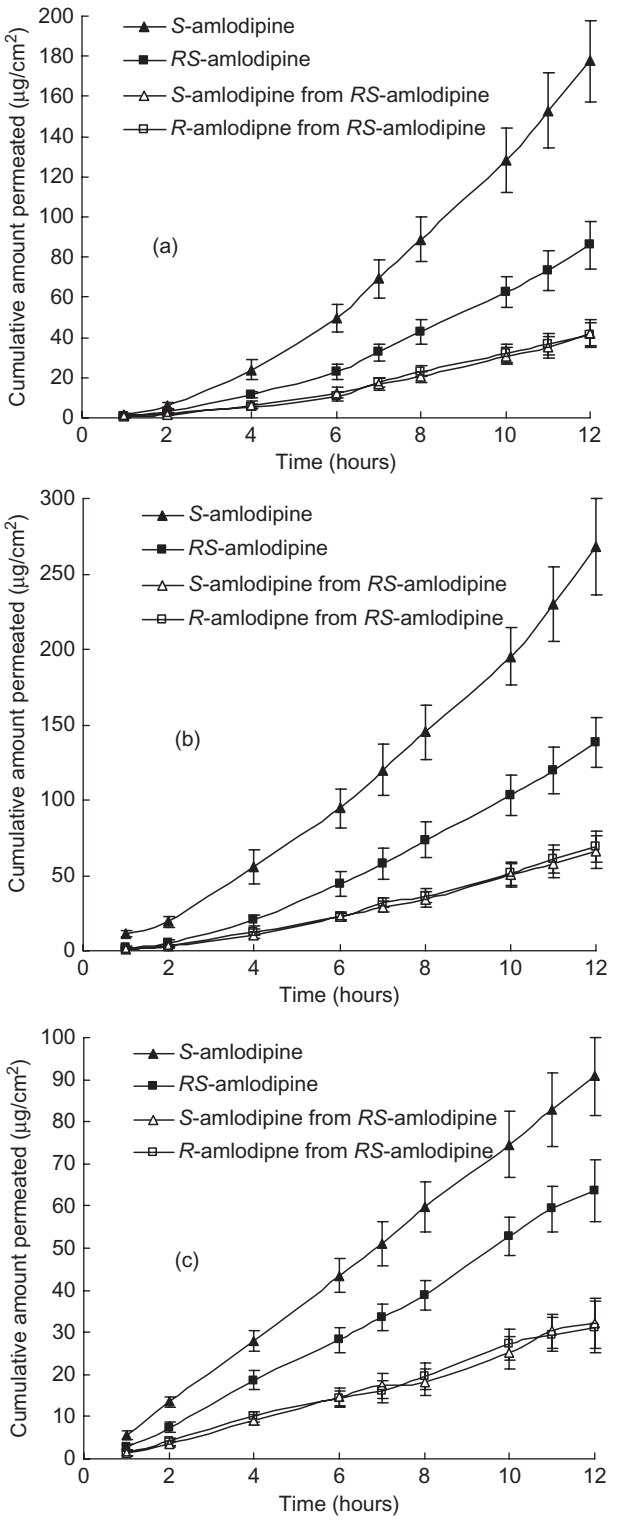

Figure 6. Permeation profiles of the racemate and enantiomers of amlodipine through the rat epidermis from the ethanol/water systems containing 0.02 M *S*-amlodipine or *RS*-amlodipine: (a) 30:70 (v/v), (b) 50:50 (v/v), (c) 75:25 (v/v).

showed that the flux values of *S*-amlodipine and *RS*-amlodipine from 30% ethanol and 50% ethanol were all higher than those of *S*-amlodipine and *RS*-amlodipine from water; specifically, the permeability enhancing ratios of 30% ethanol were 1.54 ± 0.32 and 1.43 ± 0.27 and those of 50% ethanol were 2.06 ± 0.18 and 2.04 ± 0.21. But the flux values of *S*-amlodipine and *RS*-amlodipine from 75% ethanol were all lower than those of *S*-amlodipine and *RS*-amlodipine from water, with permeability enhancing ratios of 0.56 ± 0.08 and 0.78 ± 0.11. These results suggested that 30% and 50% ethanol could enhance the permeation of *S*-amlodipine and *RS*-amlodipine through the rat epidermis, whereas 75% ethanol had the opposite effect. These results could be explained as follows. In the neat water system (without ethanol), lipophilic drugs permeated mainly through lipid pathway[31]. In low concentration ethanol (30% and 50%), lipid of the stratum corneum could be extracted and keratin of the stratum corneum could be softened, thereby promoting the permeation of a drug[32,33]. Contribution of convective flow with solvents on the skin permeation of lipophilic drugs might also be increased in low concentration of ethanol[30]. But, a high concentration of ethanol (75%) caused excessive dehydration of the skin and, therefore, had counterproductive effects on the permeation of lipophilic drugs.

Effect of terpene enhancers on permeation of S-amlodipine and RS-amlodipine

Terpenes are a group of chiral skin penetration enhancers that are derived from plant essential oils and are widely used as pharmaceutical excipients with various drugs. In this study, linalool, (−)-menthol, and (−)-limonene were chosen to study the enhancing effect of terpenes on the permeation of the racemate and enantiomers of amlodipine through the rat epidermis. To solubilize the selected penetration enhancers in the donor vehicle, 50% ethanol was chosen as the donor vehicle.

The permeation profiles of linalool, (−)-menthol, and (−)-limonene on the permeation of the racemate and enantiomers of amlodipine through the rat epidermis from 50% ethanol contained in 0.02 M *S*-amlodipine or *RS*-amlodipine were shown in Figure 7, respectively. The permeation parameters were shown in Table 3. The permeation profiles of the *S*-amlodipine and *R*-amlodipine from donor solutions containing *RS*-amlodipine were comparable with the ratios of the flux value of *R*-amlodipine and *S*-amlodipine all being about 1. These results showed that linalool, (−)-menthol, and (−)-limonene did not give rise to any enantioselective permeation. These findings were in agreement with the reported studies on metoprolol and ketoprofen.

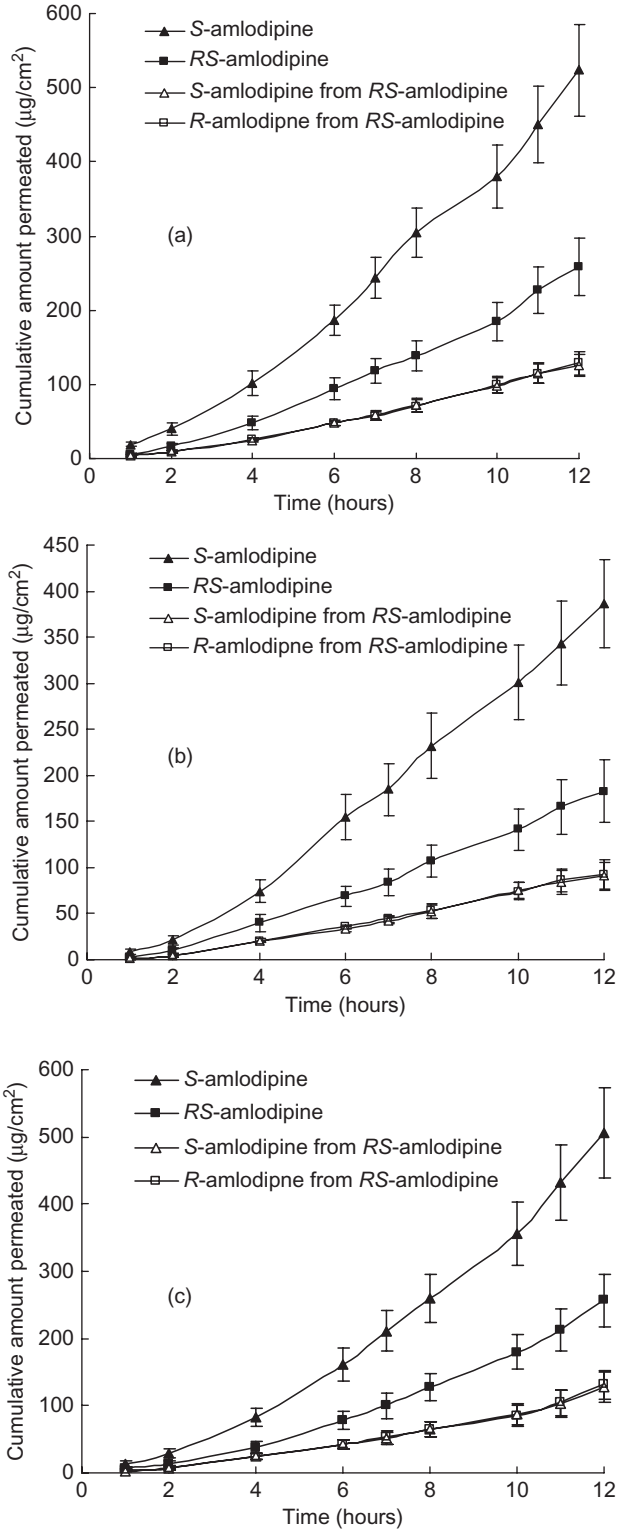

Figure 7. Permeation profiles of the racemate and enantiomers of amlodipine through the rat epidermis from 50% ethanol containing enhancer and 0.02 M *S*-amlodipine or *RS*-amlodipine: (a) 0.05 M linalool, (b) 0.05 M (–)-menthol, (c) 0.05 M (–)-limonene.

Table 3 showed that the flux values of *S*-amlodipine and *RS*-amlodipine from donor solutions containing linalool, (–)-menthol, or (–)-limonene were all higher than those of *S*-amlodipine and *RS*-amlodipine in the absence of enhancer; specifically, the permeability enhancing ratios of linalool were 1.90 ± 0.29 and 1.83 ± 0.24, those of (–)-menthol were 1.37 ± 0.16 and 1.24 ± 0.08, and those of (–)-limonene were 1.99 ± 0.17 and 1.96 ± 0.21. These observations were in agreement with the reported studies on nicardipine hydrochloride and diclofenac sodium where terpenes had permeation enhancing effect[27,34]. The mechanism of permeation enhancement of the terpene enhancers had been evaluated using DSC, FTIR, and X-ray diffraction. These studies suggested that terpenes enhanced the permeation of the drug across the skin mainly by disrupting the highly ordered intercellular packing of the stratum corneum lipids and by increasing drug diffusivity[35–37].

The fluxes *S*-amlodipine were all higher than those of the *RS*-amlodipine from donor solutions containing linalool, (–)-menthol, or (–)-limonene, with the flux ratios of *S*-amlodipine and *RS*-amlodipine being 1.98 ± 0.14, 2.11 ± 0.19, and 1.94 ± 0.18, respectively. Compared with the flux ratio (1.91 ± 0.24) of *S*-amlodipine and *RS*-amlodipine in the absence of enhancer, there was no significant difference ($P > 0.05$). These results showed no significant difference between the permeability enhancing effect of linalool, (–)-menthol, or (–)-limonene on *S*-amlodipine and *RS*-amlodipine.

Conclusion

In this study, the crystalline racemate amlodipine was a cocrystal containing equal numbers of molecules of the opposite enantiomer, with the unit cell of each crystal containing enantiomeric molecules with opposite chirality. The differences in interactions between the same homochiral molecules and those between the heterochiral molecules, and the different packing arrangements in the crystal structures led to a higher melting point, a higher enthalpy of fusion, and a lower solubility of *RS*-amlodipine compared to *S*-amlodipine.

S-amlodipine with a lower melting point and a higher solubility was found to have a higher flux than *RS*-amlodipine in the transdermal permeation study in vitro. It indicated that the higher flux of *S*-amlodipine than that of *RS*-amlodipine was attributed to the differences between physical properties of *S*-amlodipine and *RS*-amlodipine. However, the difference of amlodipine enantiomers in permeation was not found in the absence and presence of enhancers, such as linalool, (–)-menthol, (–)-limonene,

Table 3. Permeation parameters of the racemate and enantiomers of amlodipine through the rat epidermis employing the donor phase consisting of 0.02 M *S*-amlodipine or *RS*-amlodipine in 50% ethanol.

Donor composition	Permeant	J_s (μg/cm^2/h)	T_{lag} (hours)	ER_{flux}	Ratio *S/R* or *S/RS*
S-amlodipine	*S*-amlodipine	28.25 ± 3.16	2.79 ± 0.33		1.91 ± 0.24
RS-amlodipine	*RS*-amlodipine	14.83 ± 1.54	2.92 ± 0.25		
	S-amlodipine	7.22 ± 0.85	3.02 ± 0.32		1.02 ± 0.06
	R-amlodipine	7.45 ± 0.79	2.91 ± 0.28		
0.05 M Linalool + *S*-amlodipine	*S*- amlodipine	53.60 ± 6.03	2.50 ± 0.37	1.90 ± 0.29	1.98 ± 0.14
0.05 M Linalool + *RS*-amlodipine	*RS*-amlodipine	27.07 ± 2.95	2.72 ± 0.42	1.83 ± 0.24	
	S-amlodipine	13.33 ± 1.71	2.52 ± 0.38		0.96 ± 0.07
	R-amlodipine	13.85 ± 1.84	2.75 ± 0.44		
0.05 M (–)-Menthol + *S*-amlodipine	*S*-amlodipine	38.61 ± 4.32	2.08 ± 0.29	1.37 ± 0.16	2.11 ± 0.19
0.05 M (–)-Menthol + *RS*-amlodipine	*RS*-amlodipine	18.27 ± 2.17	2.11 ± 032	1.24 ± 0.08	
	S-amlodipine	9.41 ± 1.04	2.24 ± 0.37		1.01 ± 0.04
	R-amlodipine	9.36 ± 0.95	2.07 ± 0.38		
0.05 M (–)-Limonene + *S*-amlodipine	*S*-amlodipine	56.16 ± 6.17	3.29 ± 0.51	1.99 ± 0.17	1.94 ± 0.18
0.05 M (–)-Limonene + *RS*-amlodipine	*RS*-amlodipine	28.95 ± 3.83	3.50 ± 0.19	1.96 ± 0.21	
	S-amlodipine	13.62 ± 1.49	3.18 ± 0.22		0.98 ± 0.06
	R-amlodipine	13.95 ± 1.32	3.25 ± 0.36		

and ethanol, and indicated that there was no enantioselectivity in the permeation of amlodipine across rat skin.

Acknowledgments

This work was supported in part by a grant (No.30672551) to Qiang Fu from National Natural Science Foundation of China.

Declaration of interest

The authors report no conflicts of interest. The authors alone are responsible for the content and writing of this paper.

References

1. Drayer DE. (1986). Pharmacodynamic and pharmacokinetic differences between drug enantiomers in humans: An overview. Clin Pharmacol Ther, 40:125–33.
2. Islam MR, Mahdi JG, Bowen ID. (1997). Pharmacological importance of stereochemical resolution of enantiomeric drugs. Drug Saf, 17:149–65.
3. Midha KK, Mckay G, Rawson MJ, Hubbard JW. (1998). The impact of stereoisomerism in bioequivalence studies. J Pharm Sci, 87:797–802.
4. Mikus P, Marakova K, Marak J, Nemec I, Valaskova I, Havranek E. (2008). Direct quantitative determination of amlodipine enantiomers in urine samples for pharmacokinetic study using on-line coupled isotachophoresis-capillary zone electrophoresis separation method with diode array detection. J Chromatogr B Analyt Technol Biomed Life Sci, 875:266–72.
5. Wainer I. (1993). Drug stereochemistry: Analytical methods and pharmacology. New York: Marcel Dekker.
6. Reddy IK, Mehvar R. (2004). Chirality in drug design and development. New York: Marcel Dekker.
7. Rustichelli C, Gamberini MC, Ferioli V, Gamberini G. (1999). Properties of the racemic species of verapamil hydrochloride and gallopamil hydrochloride. Int J Pharm, 178:111–20.
8. Kommuru TR, Khan MA, Reddy IK. (1998). Racemate and enantiomers of ketoprofen: Phase diagram, thermodynamic studies, skin permeability, and use of chiral permeation enhancers. J Pharm Sci, 87:833–40.
9. Heard CM, Brain KR. (1995). Does solute stereochemistry influence percutaneous penetration? Chirality, 7:305–9.
10. Miyazaki K, Kaiho F, Inagaki A, Dohi M, Hazemoto N, Haga M, et al. (1992). Enantiomeric difference in percutaneous penetration of propranolol through rat excised skin. Chem Pharm Bull, 40:1075–6.
11. Benezra C, Stampf JL, Barbier P, Ducombs G. (1985). Enantiospecificity in allergic contact dermatitis. Contact Derm, 13:110–4.
12. Ahmed S, Imai T, Yoshigae Y, Otagiri M. (1997). Stereospecific activity and nature of metabolizing esterases for propranolol prodrug in hairless mouse skin, liver and plasma. Life Sci, 61:1879–87.
13. Udata C, Tirucherai G, Mitra AK. (1999). Synthesis, stereoselective enzymatic hydrolysis, and skin permeation of diastereomeric propranolol ester prodrugs. J Pharm Sci, 88:544–50.
14. Kommuru TR, Khan MA, Reddy IK. (1999). Effect of chiral enhancers on the permeability of optically active and racemic metoprolol across hairless mouse skin. Chirality, 11:536–40.
15. Heard CM, Suedee R. (1996). Stereoselective adsorption and trans-membrane transfer of propranolol enantiomers using cellulose derivatives. Int J Pharm, 139:15–23.
16. Touitou E, Chow DD, Lawter JR. (1994). Chiral [beta]-blockers for transdermal delivery. Int J Pharm, 104:19–28.
17. Roy SD, Chatterjee DJ, Manoukian E, Divor A. (1995). Permeability of pure enantiomers of keterolac through human cadaver skin. J Pharm Sci, 8:987–90.
18. Murdoch D, Heel RC. (1991). Amlodipine. A review of its pharmacodynamic and pharmacokinetic properties, and therapeutic use in cardiovascular disease. Drugs, 41:478–505.
19. Meredith PA, Elliott HL. (1992). Clinical pharmacokinetics of amlodipine. Clin Pharmacokinet, 22:22–31.
20. Helms SR. (2007). Treatment of feline hypertension with transdermal amlodipine: A pilot study. J Am Anim Hosp Assoc, 43:149–56.
21. Goldmann S, Stoltefuss J, Born L. (1992). Determination of the absolute configuration of the active amlodipine enantiomer as (–)-S: A correction. J Med Chem, 35:3341–4.

22. Arrowsmith JE, Campbell SF, Cross PE, Stubbs JK, Burges RA, Gardiner DG, et al. (1986). Long-acting dihydropyridine calcium antagonists. 1. 2-Alkoxymethyl derivatives incorporating basic substituents. J Med Chem, 29:1696–702.
23. Kumar D, Aqil M, Rizwan M, Sultana Y, Ali M. (2009). Investigation of a nanoemulsion as vehicle for transdermal delivery of amlodipine. Pharmazie, 64:80–5.
24. McDaid DM, Deasy PB. (1996). Formulation development of a transdermal drug delivery system for amlodipine base. Int J Pharm, 133:71–83.
25. Luka J, Josi D, Kremser M, Kopitar Z, Milutinovi S. (1997). Pharmacokinetic behaviour of R-(+)- and S-(-)-amlodipine after single enantiomer administration. J Chromatogr B Analyt Technol Biomed Life Sci, 703:185–93.
26. Streel B, Laine C, Zimmer C, Sibenaler R, Ceccato A. (2002). Enantiomeric determination of amlodipine in human plasma by liquid chromatography coupled to tandem mass spectrometry. J Biochem Biophys Methods, 54:357–68.
27. El-Kattan AF, Asbill CS, Kim N, Michniak BB. (2001). The effects of terpene enhancers on the percutaneous permeation of drugs with different lipophilicities. Int J Pharm, 215:229–40.
28. Duddu SP, Grant DJ. (1992). Formation of the racemic compound of ephedrine base from a physical mixture of its enantiomers in the solid, liquid, solution, or vapor state. Pharm Res, 9:1083–91.
29. Jacques J, Collet A, Wilen SH. (1981). Enantiomers, racemates, and resolutions. New York: Wiley.
30. Manabe E, Sugibayashi K, Morimoto Y. (1996). Analysis of skin penetration enhancing effect of drugs by ethanol–water mixed systems with hydrodynamic pore theory. Int J Pharm, 129:211–21.
31. Hatanaka T, Inuma M, Sugibayashi K, Morimoto Y. (1990). Prediction of skin permeability of drugs. I. Comparison with artificial membrane. Chem Pharm Bull, 38:3452–9.
32. Higuchi WI, Liu P, Ghanem AH, Song W. (1987). Mechanism of ethanol effect on the simultaneous transport and metabolism of β-estradiol in hairless mouse skin. Control Release Bioact Mater, 14:101–2.
33. Kurihara-Bergstrom T, Knutson K, DeNoble LJ, Goates CY. (1990). Percutaneous absorption enhancement of an ionic molecule by ethanol–water systems in human skin. Pharm Res, 7:762–6.
34. Arellano A, Santoyo S, Martin C, Ygartua P. (1996). Enhancing effect of terpenes on the in vitro percutaneous absorption of diclofenac sodium. Int J Pharm, 130:141–5.
35. Sinha VR, Kaur MP. (2000). Permeation enhancers for transdermal drug delivery. Drug Dev Ind Pharm, 26:1131–40.
36. Cornwell PA, Barry BW, Stoddart CP, Bouwstra JA. (1994). Wide-angle X-ray diffraction of human stratum corneum: Effects of hydration and terpene enhancer treatment. J Pharm Pharmacol, 46:938–50.
37. Williams AC, Barry BW. (1991). Terpenes and the lipid-protein-partitioning theory of skin penetration enhancement. Pharm Res, 8:17–24.